Proceedings of the 9th International Symposium on Landslides, Rio de Jameiro,
Brazil.Vol.2. pp.1079-1084. June 28- July 2. 2004

Transient stability analysis of a collapsible dam using dynamic programming combined with finite element stress state fields

C.C. Brito
J.H.F. Pereira (in memoriam)
University of Brasília, Brasília, DF, Brazil

G.F.N. Gitirana Jr.
D.G. Fredlund
University of Saskatchewan, Saskatoon, SK, Canada

ABSTRACT: This paper presents the application of the Dynamic Programming Method (DPM) combined with finite element stress fields to the analysis of stability of a collapsible earth dam during the first reservoir filling. Slip surface shape restrictions are relaxed through the use of the DPM, allowing for a more rigorous analysis of the failure mechanism. In order to perform the analysis, the DPM solver SAFE-DP was combined with the coupled hydro-mechanical finite element code COUPSO. The analysis results show that the DPM solver was capable of identifying the failure mechanisms observed in the field. Non circular critical slip surfaces were found for most of the stages. A reduction in factor of the safety with time was found. The dam is stable during the construction phase and the upstream slope fails 138 days after the first reservoir filling.

1 INTRODUCTION

Small collapsible earth dams are commonly found in the semi-arid region in north-eastern Brazil. These dams are built in order to provide a water reservoir that can accumulate precipitation from the short, wet season, providing water for agriculture and public use during the long, dry season. Because of lack of appropriate compaction equipment and water, these dams are poorly compacted, at dry of optimum, meta-stable conditions. As a result, the compacted soil suffers considerable collapse and loss of shear strength when wetted, during the first reservoir filling (Pereira, 1996). The failure mechanism is usually characterised by a wedge failure of the upstream slope, combined with piping at the downstream slope.

This paper presents the analysis of stability of a typical small collapsible earth dam. In order to perform the analysis, the DPM code SAFE-DP (Gitirana Jr and Fredlund, 2003) was combined with the fully coupled hydro-mechanical finite element code COUPSO (Pereira, 1996). The constitutive parameters used where obtained from state surfaces and a nonlinear perfect plastic elastic behaviour was assumed. Both upstream and downstream slopes were studied. The paper presents the analysis of the evolution of slip surface shape and position, and of the evolution of factors of safety during the end of construction, rapid reservoir filling, and post-filling phases. The performance of the DPM is discussed.

2 DYNAMIC PROGRAMMING METHOD

The dynamic programming method (DPM) is a general method of maximization and minimization of linear functionals (Bellman, 1957). Baker (1980) introduced the application of the DPM to the analysis of slope stability. The procedure proposed by Baker (1980) used the DPM, while retaining the Spencer (1967) assumption regarding interslice forces. Later, several researchers presented extensions of Baker's procedure, replacing the Spencer assumption by using finite element stress fields (Yamagami & Ueta , 1988; Zou et al., 1995; Pham et al., 2001, Gitirana Jr. and Fredlund, 2003).

2.1 Optimization procedure

The DPM is a general optimization procedure that can be used for determining the failure mechanism and the corresponding minimum factor of safety. As shown in Fig. 1, the slip surfaces are formed by a series of linear segment defined by stages and state points. The factor of safety can be defined in a discrete form, as follows:

$$Fs = \sum_{i=1}^{n} \tau_{f_i} \Delta L_i \Big/ \sum_{1}^{n} \tau_i \Delta L_i \qquad (1)$$

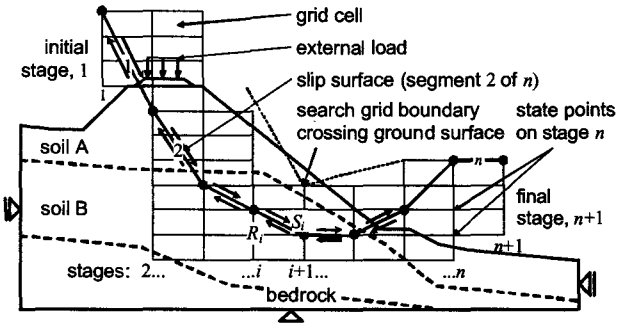

Figure 1. The analytical scheme of stability analysis using Dynamic Programming (Gitirana Jr and Fredlund, 2003).

where n = number of segments; τ_{fi} = shear strength of the soil along segment "i"; ΔL_i = length of segment "i"; and τ_i = acting shear stress along segment "i". The functional Fs cannot be minimised using the DPM because the method is not applicable for non-additive functionals. Baker (1980) showed that the minimisation of Fs can be achieved by minimising the following auxiliary functional:

$$G = \sum_{i=1}^{n} \left(\tau_{f_i} - F_s \tau_i\right) \Delta L_i \tag{2}$$

The minimisation of G is performed using the principle of optimality (Bellman, 1957). According to the principle of optimality, the optimal function at a posterior stage, $H_{i+1}(j)$, is function of the optimum function at the prior stage, $H_i(k)$, as follows:

$$H_{i+1}(j) = \min\left[H_i(k) + DG_{i+1}(j,k)\right] \tag{3}$$

where $DG_{i+1}(j, k)$ is the 'cost' of passing between two state points at consecutive stages. The value of the optimal function at the initial stage ($H_1(k) = 1$) is equal to zero at any state point. At the last stage, the optimal function corresponds to the minimum value o G, as follows:

$$H_{n+1}(j) = G_{\min} = \sum_{i=1}^{n} \left(R_i - F_s S_i\right) \tag{4}$$

where R_i = resisting force along the segment "i"; and S_i = shear force along the segment "i". Once the optimal function at the last stage is determined, the optimum path is found by connecting the optimal state points, traced back from the final to the last stage. The critical slip surface corresponds to the optimum path.

As can be seen in Eq. 1, the optimization procedure is nonlinear. An initial value for Fs must be assumed and the computation must be repeated until the value of Fs converges, for a given error tolerance.

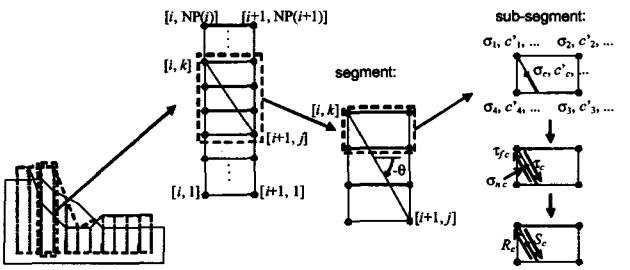

Figure 2. Optimum variables on a segment connecting two state points (Gitirana Jr and Fredlund, 2003).

2.2 Computation of the stresses used in the analysis

The shear strength along any segment "i" can be defined based on the shear strength envelope and using the stress state variables. The stress state field for two orthogonal plane oriented in the x- and y-directions (σ_x, σ_y, and τ_{xy}) can be obtained using the finite element method. The normal stress, σ_θ, and the shear stress, τ_θ, acting on any segment sloped at an angle θ (see Fig. 2) can be calculated based on the stress state field defined by σ_x, σ_y, and τ_{xy}, using the following equations:

$$\sigma_\theta = \sigma_x sen^2\theta + \sigma_y \cos^2\theta - \tau_{xy} sen2\theta \tag{5}$$

$$\tau_\theta = \tau_{xy}\left(sen^2\theta - \cos^2\theta\right) - \frac{\left(\sigma_y - \sigma_x\right)}{2} sen2\theta \tag{6}$$

3 COUPLED DIFFERENTIAL EQUATIONS GOVERNING THE HYDRO-MECHANICAL SOIL BEHAVIOUR

The stress state field used for the stability analysis of a collapsible dam has been calculated using the finite element code COUPSO (Pereira, 1996). The program COUPSO solves the equilibrium and water conservation equations for two-dimensional plane-strain conditions in a fully coupled way. COUPSO was developed for the analysis of the behaviour of unsaturated soils, the saturated condition being a particular condition. The constitutive models and parameters are based on the state surface concept (Matyas and Radhakrishna, 1968) and on a nonlinear elastic, perfect plastic behaviour. State surfaces for void ratio, degree of saturation, hydraulic conductivity, and Poisson ratio and the shear strength envelope are defined using the stress state variables; namely, net total stress, $(\sigma - u_a)$, and matric suction, $(u_a - u_w)$. The flow of air is neglected, based on the assumption that the air phase is continuous and in contact with the atmosphere.

3.1 Static equilibrium

The partial differential equations governing static equilibrium can be obtained by considering the equilibrium of forces acting on a representative elemental volume of soil (REV). The stresses within the differential equations can be replaced by strains using the stress-strain relationship (generalised Hook's law). The following equations are obtained for the x- and y-directions, respectively:

$$\frac{\partial}{\partial x}\left(c_{11}\frac{\partial u}{\partial x}+c_{12}\frac{\partial v}{\partial y}\right)+\frac{\partial}{\partial y}\left[c_{33}\left(\frac{\partial u}{\partial x}+\frac{\partial v}{\partial y}\right)\right] - d_s^x\frac{\partial(u_a-u_w)}{\partial x}+b_x=0 \quad (7)$$

$$\frac{\partial}{\partial x}\left[c_{33}\left(\frac{\partial u}{\partial y}+\frac{\partial v}{\partial x}\right)\right]+\frac{\partial}{\partial y}\left(c_{12}\frac{\partial u}{\partial x}+c_{22}\frac{\partial v}{\partial y}\right) - d_s^y\frac{\partial(u_a-u_w)}{\partial x}+b_y=0 \quad (9)$$

where u and v = displacements in the x- and y-directions, respectively; $c_{11} = c_{22} = E(1-\mu)/(1+\mu)(1-2\mu)$; $c_{12} = E\mu/(1+\mu)(1-2\mu)$; $c_{33} = E/2(1+\mu)$; E = Young modulus; μ = Poisson's ratio; $d_s^x = c_{11}[1/H_x+\mu/(1-\mu)H_y+\mu/(1-\mu)H_z]$; $d_s^y = c_{11}[\mu/(1-\mu)H_x+1/H_y+\mu/(1-\mu)H_z]$; H_i = elastic modulus for the soil skeleton at the i-direction associated with matric suction, $(u_a - u_w)$, changes; u_a = pore-air pressure; u_w = pore-water pressure; and b_i = body forces in the i-direction.

3.2 Water mass conservation

The partial differential equation governing two-dimensional flow and conservation of water can be obtained by considering the flow of water in and out of a REV of soil and using Darcy's law for water flow. The equation obtained is as follows:

$$\beta_{w1}\frac{\partial\varepsilon_v}{\partial t}+\beta_{w2}\frac{\partial(u_a-u_w)}{\partial t}=\nabla\left[k\nabla\left(\frac{u_w}{\gamma_w}+y\right)\right] \quad (9)$$

where $\beta_{w1} = (m_1^w/m_1^s)$; $\beta_{w2} = m_2^w - (m_1^w m_2^s/m_1^s)$; $m_1^w = [2(1+\mu)/E_w]$; $m_2^w = [1/H_w - (E/H)/E_w]$; $m_1^s = 2(1+\mu)(1-2\mu)/E$; $m_2^s = [1/H_x + 1/H_y + 2\mu/H_z]$; E_w = volumetric modulus for the water phase with respect to changes in net mean stress, σ-u_a; H_w = volumetric modulus for the water phase with respect to changes in matric suction; ε_v = total volumetric strain; ∇ = divergent operator; k = hydraulic conductivity; γ_w = unit weight of water; and y = elevation.

4 ANALYSIS OF STABILITY OF A SMALL METASTABLE EARTH DAM

The hypothetical earth dam analysed is representative of the typical small metastable dams encountered in the semi-arid region of north-eastern Brazil. The following sections will present the soil properties used in the analyses, the problem geometry, initial and boundary conditions, and the results of the stability analyses. The results presented herein will focus on the stability analyses results obtained using the program SAFE-DP and using the stress state finite element fields obtained. The results of the coupled stress and water flow analyses using the program COUPSO are presented in detail by Brito (2003).

4.1 Soil properties

The soil properties adopted correspond to a residual soil from the Ceará group that has a silty sand texture (Pereira, 1996). The soil properties were experimentally determined using triaxial, oedometric and direct shear apparatuses, with and without matric-suction control. The detail regarding the laboratory apparatuses and procedures, and the result of this experimental program are presented in detail by Pereira (1996) and Pereira and Fredlund (2000).

The soil properties summarised herein are based on tests performed under monotonic wetting paths with matric suction varying, in stages, from 370 to 0 kPa. Pereira (1996) presented mathematical functions that were fitted to the experimental results. These functions are based on the stress state variables $(\sigma - u_a)$ and $(u_a - u_w)$. The mathematical functions employed are capable of fitting the experimental data obtained, are continuous, and have continuous derivatives. The functions used to define the state surfaces for void ratio, e, and degree of saturation, S, are as follows:

$$e = e_u + \frac{e_f - e_u}{\left[1+\left(\frac{(u_a-u_w)}{c}\right)^b\right]} \quad (10)$$

$$S = S_0 + \frac{(1-S_0)}{\left\{1+\left(\frac{(u_a-u_w)}{c^m}\right)^d\right\}} \quad (11)$$

where $e_u = 0.7697\text{-}0.0073\ln(\sigma_m - u_a)$ is the void ratio for the pre-collapse phase; $e_f = 0.752+\{[-0.142/(1+((\sigma_m - u_a)/75)^{-3.5}]\}$ is the void ratio for the

post-collapse phase; $b = 39.01(\sigma_m - u_a)^{-0.6103}$ is a parameter the controls the shape of the collapse phase; $c = 0.00094(\sigma_m - u_a)^2 + 0.07465(\sigma_m - u_a) + 11$ is a parameter that corresponds to the matric suction at the middle of the collapse phase; $(\sigma_m - u_a)$ = net normal mean stress; $S_0 = 0.375$ is the initial saturation; $d = 0.9769$ is a parameter the defines the slope of the wetting curve at the collapse phase; and $c^m = 20$ is a parameter that corresponds to the matric suction at the middle of the collapse phase.

The experimental results for hydraulic conductivity were fitted by Pereira (1996) using the following function:

$$k_w = k_p \left(\frac{\Psi_{cr}}{(u_a - u_w)} \right)^{\lambda} \tag{12}$$

where $k_p = -1.4*10^{-7}+6.26*10^{-8}\ln(\sigma_m - u_a)$ gives the change in hydraulic conductivity for changes in total mean stress; $\psi_{cr} = 3.0$ is the air-entry value; $\lambda = 2.1$ is an empirical constant.

The shear strength envelope was obtained by Pereira (1996) using a direct shear apparatus with matric suction control. The matric suction values varied from 100 to 0 kPa since the contribution of higher values of matric suction was found to be negligible. The following function was used to represent the shear strength envelope:

$$\tau_{ff} = a_1 + b_1(\sigma - u_a) + c_1(u_a - u_w) + d_1(\sigma - u_a)(u_a - u_w)^p \tag{13}$$

where $a_1 = 5.0$ is the effective cohesion intercept; $b_1 = 0.1944$ is the tangent of the effective friction angle; and $c_1 = 0.3238$, $d_1 = 0.09319$ and $p = 4.307\text{x}10^{-7}$ are fitting parameters.

4.2 Problem geometry, boundary and initial conditions

Figure 3 presents the problem geometry and finite element mesh used for the analysis of the construction, rapid reservoir filling, and post-filling phases. The construction phase was simulated using 5 layers and considering a linear elastic behaviour with $\mu = 0.3$ and $E = 5800$ kPa. The only acting load during the construction phase was the body load corresponding to the unit weight of the soil (γ_{nat} = 14.75 kN/m^3). The boundary condition at the lower boundary corresponds to a rigid foundation, with no relative slippage (no displacements in the x- and y-directions). Pore-water pressure changes during the construction phase were neglected.

A matric suction of 370 kPa and the stresses obtained from the construction phase simulation were assumed as the initial condition for the simulation of the rapid reservoir phase. The value of initial matric suction was obtained by Pereira (1996), using on null tests. The same value of matric suction and the stresses obtained from the rapid reservoir filling analysis were used as initial condition for the post-filling phase simulation. The water flow boundary conditions assumed for the post-filling analysis are presented in Fig. 3. No water infiltration and pore-water pressure changes were allowed during the rapid filling. The time discretisation consisted of an initial time step of 17 days, followed by smaller time steps of 0.2 days. A larger initial time step was required in order to prevent numerical instability.

4.3 Presentation of results and discussion

Figures 4 and 5 show the evolution of the critical slip surface shape and position for the upstream and downstream slopes, respectively. It can be observed that the critical slip surfaces and factors of safety of the upstream and downstream slopes are identical for the end of construction phase, as expected.

The critical slip surface for the upstream slope after the rapid reservoir filling phase is slightly deeper than the critical slip surface for the end of construction phase. This is due to the higher confining stresses near the upstream slope as a result of the reservoir load. Another effect of the reservoir loading is a considerable increase in the factor of safety, due to the higher shear strength mobilization due to friction. Considering that the increase in confining stresses due to reservoir load decrease with increasing distances from the upstream slope, the relative results obtained for the end of construction and rapid filling phases are correct. The critical slip surface and factor of safety for the downstream slope after the rapid reservoir filling phase did not suffer any significant change.

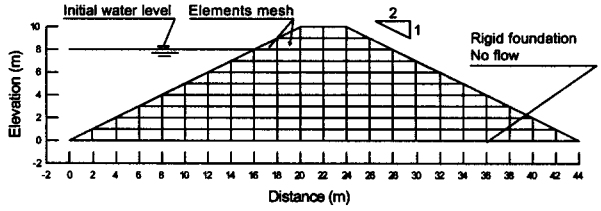

Figure 3. Cross-section of the dam, finite element mesh, and boundary conditions.

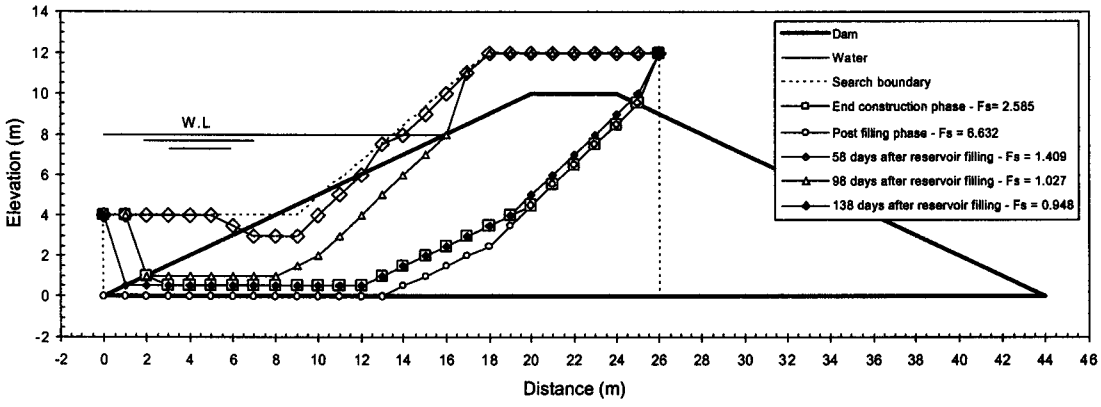

Figure 4. Stability analysis results for the upstream slope.

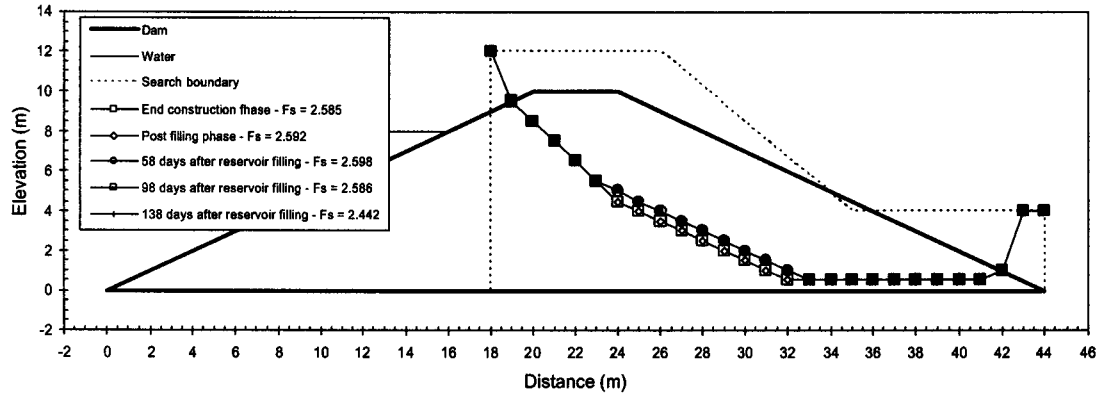

Figure 5. Stability analysis results for the downstream slope.

Figure 4 and 5 also show the critical slip surfaces for the post filling phase. The wetting front advance causes differential settlement of the dam. As a result, the stress distribution changes in order to accommodate such settlements. A relatively shallow upstream critical slip surface was found for 58 days after the reservoir filling. This result is in agreement with the position of the wetting front and the corresponding decrease in shear strength at that region. The critical slip surface for the downstream slope was not significantly changed at this stage.

The upstream critical slip surface for 98 days after the reservoir filling is deeper that the previous slip surface (for 58 days). The slip surface has a shape that deviates considerably from a circular shape. The deepening of the critical slip surface and the reduction in factor of safety is due to the further advance of the wetting front. The downstream slope was again, not significantly affected by the wetting front that is still limited to the region near the upstream slope.

The upstream critical slip surface obtained for 138 days after the reservoir filling correspond to the stage when the dam theoretically fails ($Fs < 1$). The critical slip surface obtained is deeper than the previous surfaces, following the advance of the wetting front. The slip surface shape deviates considerably from a circular shape and is controlled by the position of the rigid dam foundation. No significant change in the downstream slope factor of safety and critical slip surface was observed. The little reduction in factor of safety is due to the redistribution of stresses due to differential settlements. Figure 6 summarises the factor of safety evolution discussed above.

5 CONCLUSIONS

This paper presented the analysis of stability of a collapsible dam using the Dynamic Programming Method (DPM) combined with finite element stress state fields. Stability analyses where performed for the end of construction, rapid reservoir filling, and post filling phases. The stress state fields were obtained through a fully coupled stress and water flow analysis using the computer code COUPSO. The combination of the DPM and the coupled analysis allowed for the relaxation of slip surface shape restrictions and a relatively rigorous modelling of the soil hydro-mechanical behaviour.

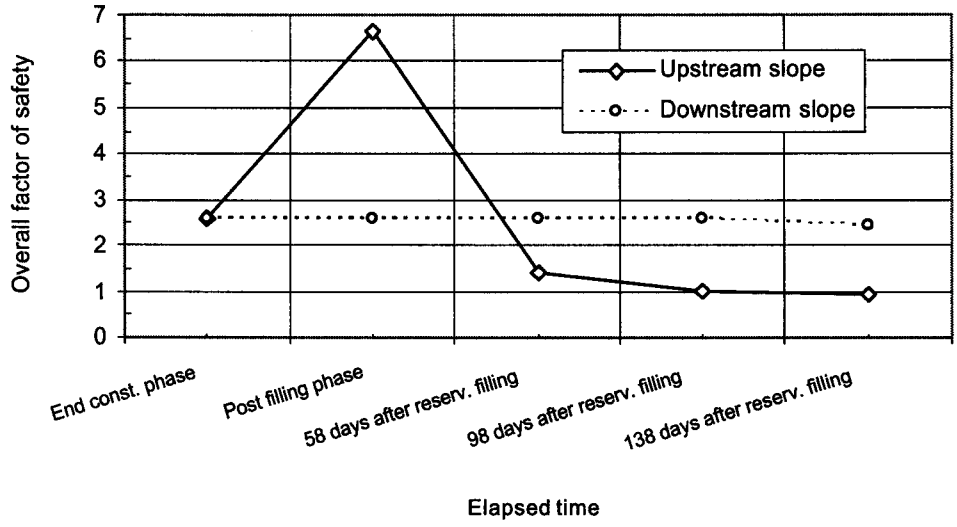

Figure 6. Evolution of the factor of safety with time for the downstream and upstream slopes.

In spite of the complex stress state fields obtained for the metastable dam during the transient wetting, the Dynamic Programming code SAFE-DP was capable of identifying the rupture mechanism observed in the field. The factor of safety results are also in quantitative agreement with the expected values. The collapsible dam is stable during the construction and rapid reservoir filling phases and becomes unstable as the wetting front advances though the dam. The results indicate that a factor of safety below 1 is reached 138 days after the reservoir filling.

6 ACKNOWLEDGMENTS

The authors would like to thank the "Conselho Nacional de Desenvolvimento Científico e Tecnológico – CNPq, Brazil, " for financial support.

7 REFERENCES

Baker, R. (1980). Determination of the critical slip surface in slope stability computations. International Journal for Numerical and Analytical Methods in Geomechanics, 4: 333-359

Bellman, R. (1957). Dynamic Programming. Princeton University Press, Princeton, New Jersey, USA, 1 vol., 337 p.

Brito, C.C. (2003). Programação Dinâmica Aplicada a Análise de Estabilidade de Taludes Não Saturados. Pub. G.DM 109A/03, Dept. de Eng. Civil, UnB, Brasília, DF, 139 p. (in Portuguese)

Gitirana Jr, G.F.N., Fredlund, D.G. (2003). Analysis of transient embankment stability using the dynamic programming method. 56th Canadian Geotechnical Conference, Winnipeg, Canada. 808-814.

Matyas, E. L. & Radhakrishna, H. S. (1968). Volume change characteristics of partially saturated soils. Geotechnique, 18: 432-448

Pereira, J. H. P. (1996). Numerical Analysis of the Mechanical Behavior of Collapsing Earth Dams During First Reservoir Filling. PhD Thesis, University of Saskatchewan, Saskatoon, Canada, 449 p.

Pereira, J.H.F. & Fredlund, D.G. (2000). Volume change behavior of collapsible compacted gneiss soil. Journal of Geotechnical and Geo-Environmental Engineering – ASCE. 126(10): 907-916.

Pham, H. T. V., Fredlund, D. G. & Gitirana Jr., G. (2001). Slope stability analysis using dynamic programming combined with finite element stress analysis. International Conference on Management of the Land and Water Resource, MLWR, Vietnan.